Structural, Thermal, Optical, Mechanical and Morphological Properties of ABS/RGO with DBDPE Nanocomposites

İBRAHIM KARTERI*[a,b], MUSTAFA ÖZYEŞILDAĞ[b]

[a]*Department of Energy Systems Engineering, Faculty of Elbistan Engineering, Kahramanmaraş Istiklal University, Kahramanmaraş, Turkey*

[b]*Materials Science and Engineering Department, Kahramanmaraş Sütçü Imam University, Kahramanmaraş, Turkey*

ABSTRACT

This study aims to provide a comprehensive account of chemically reduced graphene oxide (RGO) and decabromodiphenyl ethane (DBDPE) filled acrylonitrile-butadiene-styrene (ABS) multifunctional filaments for fused deposition modeling (FDM) applications. ABS/RGO with DBDPE nanocomposites (ABS-GDM) were fabricated by single-screw extrusion at a diameter of 1.75 mm. The proportion of RGO and DBDPE for the ABS-GDM filaments was set to 0.75 wt%. The properties of the ABS-GDM were determined using optical, mechanical, thermal, and morphological characteristics (using scanning electron microscopy). A three-dimensional (3D) model was successfully printed using the developed ABS-GDM filaments for FDM 3D printing. These ABS-GDM have the potential to be used in FDM 3D printing. Considering the optical band gap of the nanocomposites, they can also be used in optoelectronic devices and sensor applications. Also, the vertical combustion standard testing results showed that ABS-GDM filaments can be flame retardant.

KEYWORDS: *Nanocomposite filament, Nano-structured graphene, FDM, ABS.*

1. INTRODUCTION

In the last few years, there has been a growing interest in additive manufacturing (AM) technology, which is a layer-by-layer manufacturing method based on computer-aided design. Many manufacturing organizations usually use powder or wire materials for AM technologies[1-4]. AM technology is of interest

J. Polym. Mater. Vol. **38,** No. 1-2, 2021, 167-177

Correspondence author e-mail: ibrahimkarteri@gmail.com
DOI : https://doi.org/10.32381/JPM.2021.38.1-2.13

in academic and industrial fields [1, 5-6]. The most commonly used 3D printing technology among AM technologies is fused deposition modeling (FDM) [8]. Polymers are used in FDM, which liquify upon application of heat and solidify when cooled. In FDM machines, materials are injected through indexing nozzles onto a platform. The nozzles trace the cross-section pattern for each layer with thermoplastic material, which solidifies before the application of the next layer. The process is repeated until the model is complete [9].

Polymer/graphene composites have been extensively investigated owing to their flame-retardant, physical, mechanical, optical properties [10-12]. Graphene is the basic structural unit of some carbon allotropes, including graphite, carbon nanotubes, and fullerenes[10,12]. Recently, thermoplastic polymers such as acrylonitrile-butadiene-styrene (ABS), polylactic acid (PLA), polycaprolactone (PCL), and polycarbonate (PC) have been used in FDM [13-15].

Many other academic articles related to the successful production of graphene-doped polymer-based nanocomposites have been reported in the literature[16-24]. Caminero et al. used graphene-reinforced polymer composite materials[16-18].In addition, the interlaminar binding and impact performance of 3D printed samples were also investigated. The effects of graphene supplementation and structural behavior were also analyzed. The addition of graphene into polymer-based composite materials, while maintaining their flexibility, improves the mechanical strength of the composites, in addition to their electrical and thermal properties [19-24].

In the present study, ABS-GDM were fabricated for FDM. The optical, mechanical, thermal, and structural properties of the ABS-GDM were analyzed. Also, the ABS-GDM filaments was successfully printed with the FDM device. The obtained ABS-GDM structures were suitable for large-scale FDM and optoelectronic applications.

2. MATERIALS AND METHODS

DBDPE and RGO powders were used in this experiment as additive materials, and ABS powder as the base polymer. The materials were provided by Graf Nano Technological Materials Industry and Trade Ltd. Co. RGO was obtained by reduction of graphene oxides (GO) synthesized by modified Hummers method. As we reported before in detail [25,26], the GO and RGO (conductivity >600 S/m, solubility water: insoluble, flake size 0.1-10 μm) were synthesized as powder. The ABS-GDM with 0.75 wt% RGO and 0.75 wt% DBDPE were prepared. The EDX analysis of the obtained RGO was analyzed. Fig. 1 shows EDX spectra of the RGO and the chemical structures of the RGO and DBDPE, used as additive materials.

ABS was dry-mixed mechanically with RGO and DBDPE powders and then melt-compounded using a single-screw extruder to avoid the use of a solvent system. The ABS-GDM were produced as pellets. Extruder machine was used for filament production. Fig. 2 shows the extrusion process setup for the ABS-GDM filaments manufacture. The extruder (power, 5.5 kW) has a diameter of 40 mm and cooling bath, band haul off machine (1.1 kW), pneumatic cutter and auto winding machine. To produce ABS-GDM filaments, the extrusion temperatures were maintained at 160°C to 210°C from the hopper to the die. The obtained ABS-GDM pellets poured into the feeder of the extruder machine. Rotational speed of the feeder set to 8 rpm. Extrusion temperatures were controlled by five independent heating zones. The obtained ABS-GDM filaments dived into cooling bath (20°C) for solidification. Thus, 1.75 mm diameter ABS-GDM filaments were produced by controlling the speed of the band haul off machine.

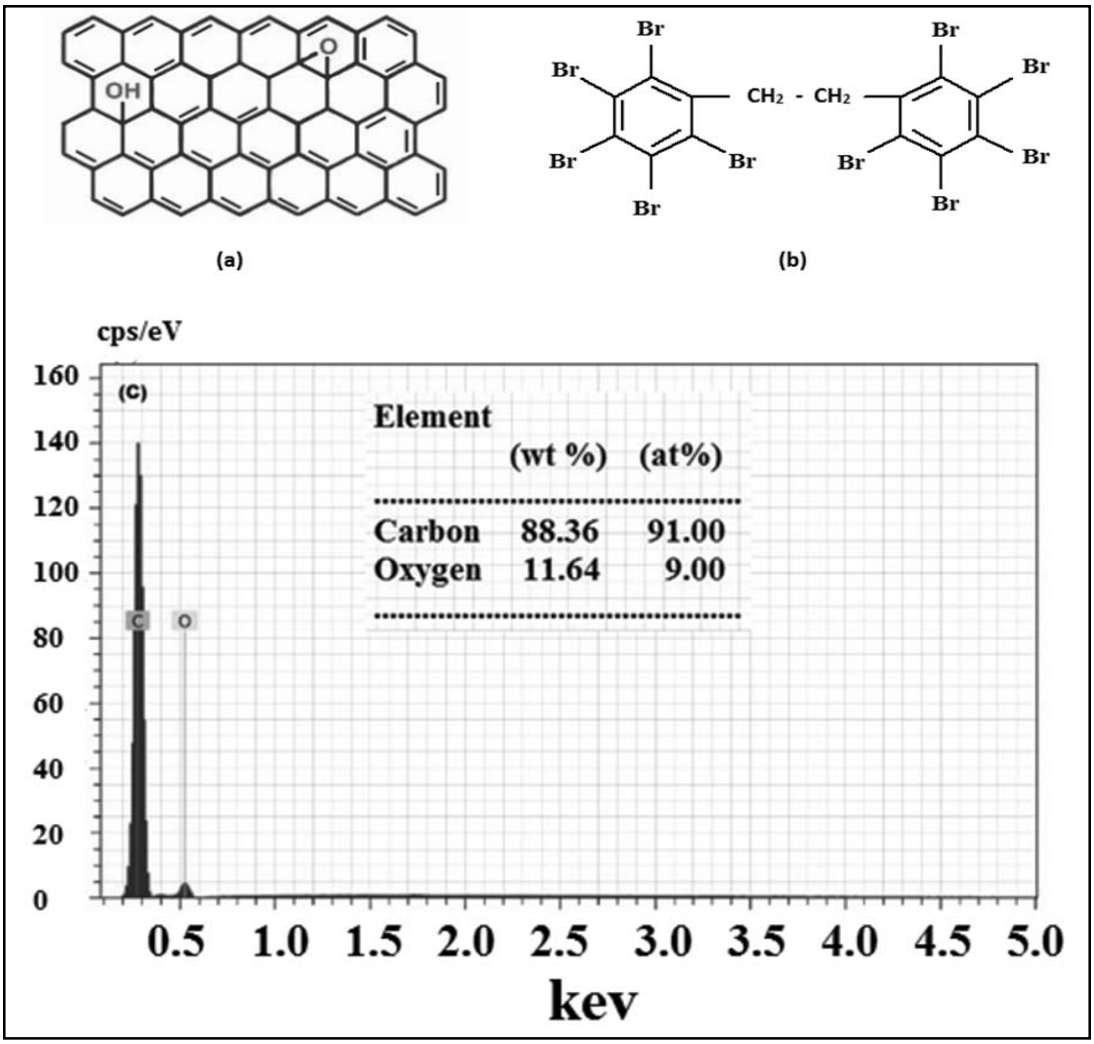

Fig. 1. Chemical structures of (a) RGO and (b) DBDPE (c) EDX spectra of the RGO.

For optical measurements of the ABS-GDM, the glass substrates were chemically cleaned in acetone and deionized water for 15 min. Then, the glass substrates were exposed to an oxygen plasma cleaner to make the surface hydrophilic and dried. ABS-GDM suspensions with concentrations of 0.015, 0.025, and 0.050 g/ml of the ABS-GDM were prepared with acetone. The prepared a-ABS-GDM (0.050 g/ml), b-ABS-GDM (0.025 g/ml), and c-ABS-GDM (0.015 g/ml) suspensions were stirred at 25°C for 2 h so as to yield clear and homogenous suspensions. To prepare the ABS-GDM films, the glass was coated with drop coating method. Then, it was dried at 50°C for 10 min.

UV-VIS spectroscopy was performed using a spectrophotometer (Shimadzu UV 1800). Fourier transform infrared (FTIR) spectroscopy measurements were conducted using an FTIR spectrometer (Perkin Elmer Spectrum). The thermal behavior of the ABS and the obtained ABS-GDM filaments was investigated by

Fig. 2. The extrusion process setup for the ABS-GDM filaments manufacture.

means of differential scanning calorimetry (DSC) using the Perkin Elmer DSC 4000 at a heating rate of 10°C/ min under air. Zeiss Evo scanning electron microscope (SEM) was operated to take surface morphology image of the RGO, DBDPE, ABS and ABS-GDM. The EDX analysis of the ABS-GDM was analyzed using Zeiss Evo LS10 SEM attached with Bruker Quantax EDS.

For mechanical and the vertical combustion standard testing, samples were prepared with the ABS-GDM pellets by a hot press, having a size of 200 x 40 x 10 mm (ASTM D790) and 127 x 12.7 x 2 mm (UL-94), respectively. The mechanical behavior of the produced composite materials was studied using a computer linked to the ZwickRoell/Z100 device. A flexural test was carried out in the three-point bending test using ZwickRoell/Z100 device according to ASTM D-790. From the obtained standard force-deformation data, the flexural strength and the flexure modules values of the ABS and ABS-GDM specimens were evaluated with the software program of the ZwickRoell/Z100.

3. RESULTS AND DISCUSSION

Considering the cost and viscosity of the ABS-based nanocomposite filaments with RGO and DBDPE for 3D printing processes, the ABS-GDM had a RGO content of 0.75 wt% and a DBDPE content of 0.75 wt%. The EDX spectra of the RGO are in Fig. 1 (c). It indicates the presence of C (88.36 wt%), O (11.64wt%) elements for the RGO.

The thermal behavior of the obtained ABS-GDM filaments was determined using a DSC with continuous heating at a rate of 10 °C /min. Fig. 3 outlines the corresponding DSC traces from the ABS and ABS-GDM filaments. The pure ABS and ABS-GDM filaments exhibit similar thermal crystallization behavior starting with a distinct glass transition temperature (T_g). Recently, the author in has found similar

crystallization behavior for ABS-GDM materials[13]. The glass transition temperature (T_g) was observed at 103°C and 104°C for ABS and ABS-GDM filaments, respectively.

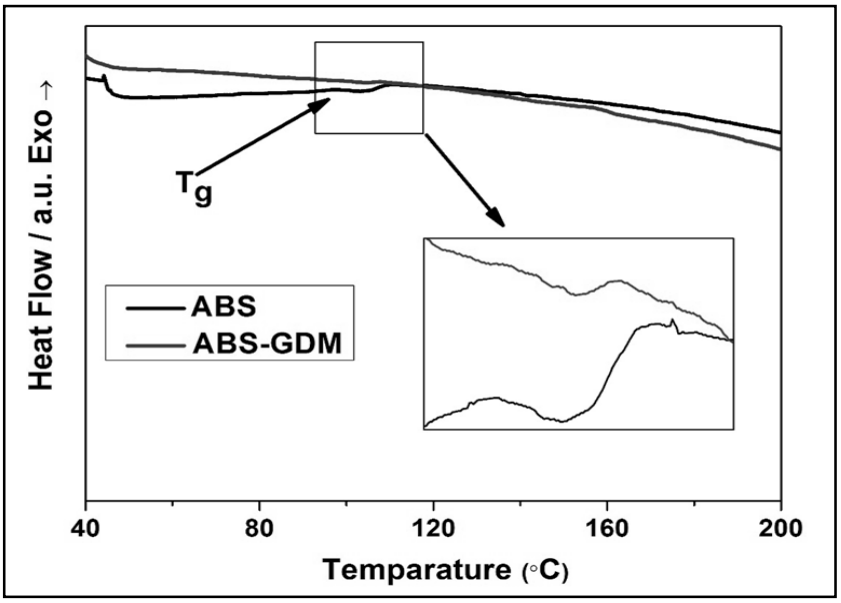

Fig. 3. Continuous DSC traces of the ABS and ABS-GDM.

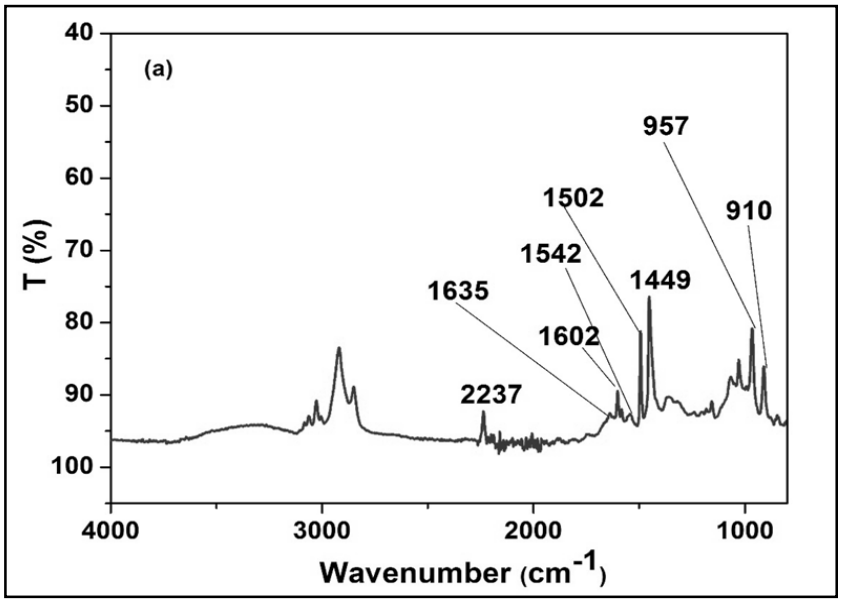

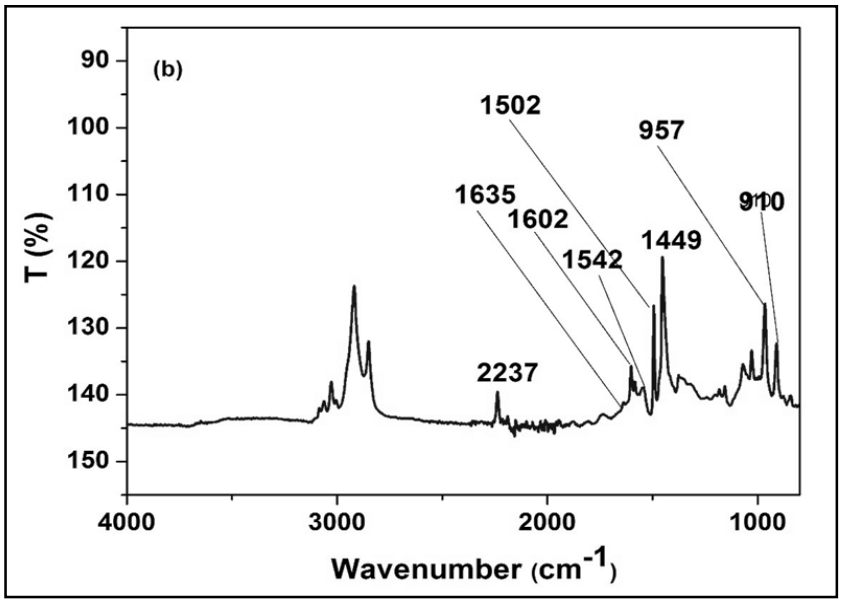

Fig. 4. Fourier transform infrared (FTIR) spectra of (a) ABS and (b)ABS-GDM.

Fig. 4 shows the Fourier Transform Infrared (FTIR) spectra of (a) ABS and (b) prepared ABS-GDM. The FTIR spectra revealed the existence of (2237 cm^{-1}) CN stretching from acrylonitrile, (1635 cm^{-1}) the C = C stretching mode of poly(butadiene), (1602, 1542, and 1502 cm^{-1}) the C = C stretching mode of the aromatic ring in styrene, (1449 cm^{-1}) the scissoring mode of the CH_2 groups, and (957 and 910 cm^{-1}) the C-H deformation for hydrogen atoms attached to the alkenic carbons in poly (butadiene) for ABS materials, as seen in Fig. 4 (a). For the ABS-GDM, a similar observation can be made, as shown in Fig. 4 (b). Similar results were reported in the literature by [27] and [28] for ABS materials. The results of this study showed that both ABS and ABS-GDM have the same peaks in their FTIR spectra. No clear peaks of the RGO and DBDPE were observed in the FTIR spectra of the ABS-GDM. However, the peak intensity of the ABS-GDM increased. This might be the result of RGO and DBDPE additives.

Fig. 5. shows SEM images of the (a) RGO (b) DBDPE (c) ABS (d) ABS-GDM nanocomposites. From the images, it can be seen that the structure of the material was not subjected to any processing. The morphology of the prepared ABS-GDM was analyzed through SEM and the images are shown in Fig. 5 (d). The results indicate that the ABS-GDM display existence and homogenous distribution of RGO and DBDPE.

Mechanical properties of ABS and the prepared ABS-GDM were tested as an average value of at least two replicates (at room temperature). From the data measured with the ZwickRoell/ Z100 device, standard force-deformation curves of ABS and ABS-GDM specimen are presented in Fig. 6. Using typical force-deformation

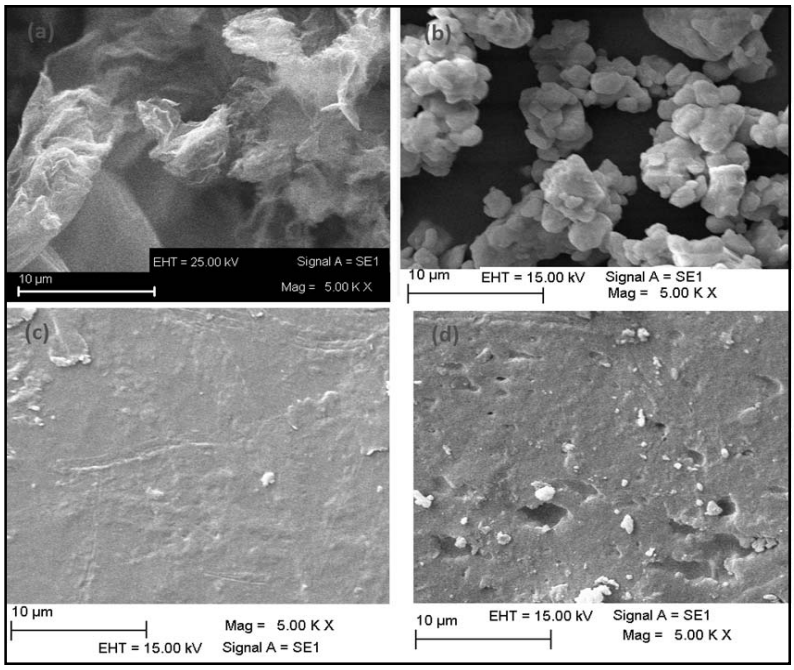

Fig. 5. SEM images of (a) RGO (b) DBDPE (c) ABS (d) ABS-GDM.

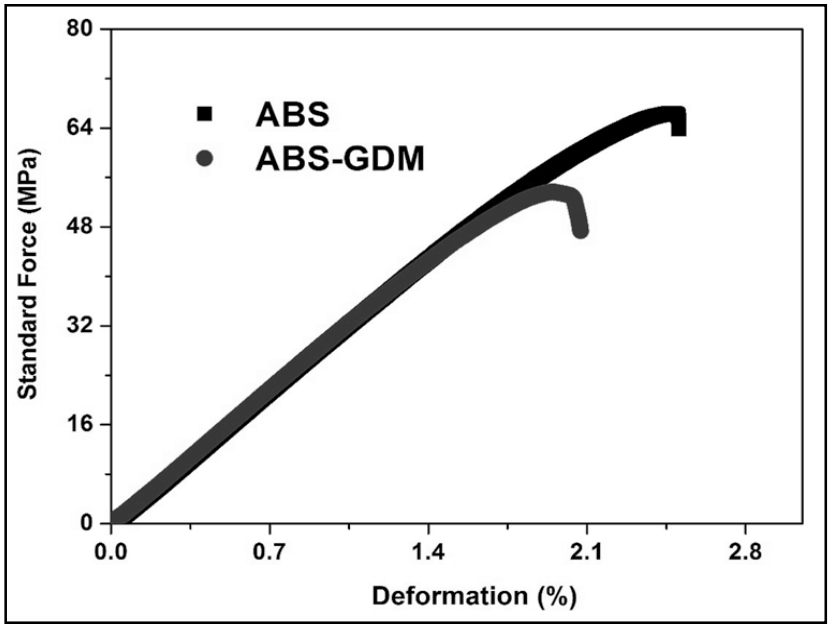

Fig. 6. Standard force-deformation curves of ABS and ABS-GDM specimens.

curves, the flexural strength and the flexure modules values of the ABS and ABS-GDM specimens were determined according to ASTM D790 using the device's software program. The flexural strength values of pure ABS and ABS-GDM were determined to be 67.53 MPa and 53.74 MPa, respectively. The flexure modulus of pure ABS and ABS-GDM was found to be 3018.48 MPa and 3051.41 MPa, respectively. The flexural strength decreases with increase in the load on RGO and DBDPE. The flexure modulus increased with the loading on RGO and DBDPE. The results show that the mechanical properties of ABS with additive materials are different.

The vertical combustion standard level of pure ABS and the ABS-GDM were determined to be no rating (NR) and V2, respectively. The vertical combustion results show that ABS-GDM filaments is an effective flame retardant with added RGO and DBDPE additives.

Fig. 7(a) shows the absorption spectra of the prepared ABS-GDM with different suspension concentrations at room temperature. The spectra of the a-ABS-GDM, b-ABS-GDM, and c-ABS-GDM structures show a strong maximum absorption band around 247 nm. As shown in the figure, the absorption of c-ABS-GDM is slightly lower than that of the a-ABS-GDM composites. It is also displayed in Fig. 7(a), that the absorbance decreases with decreasing amounts of additive material in ABS-based composites. Several authors have presented some results in [29] and [30].

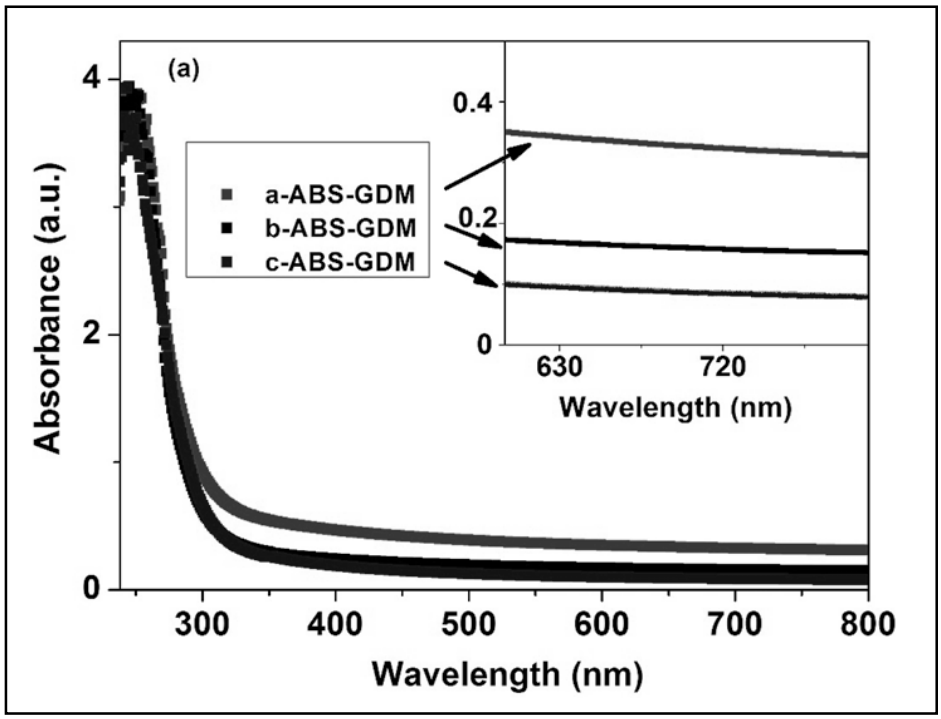

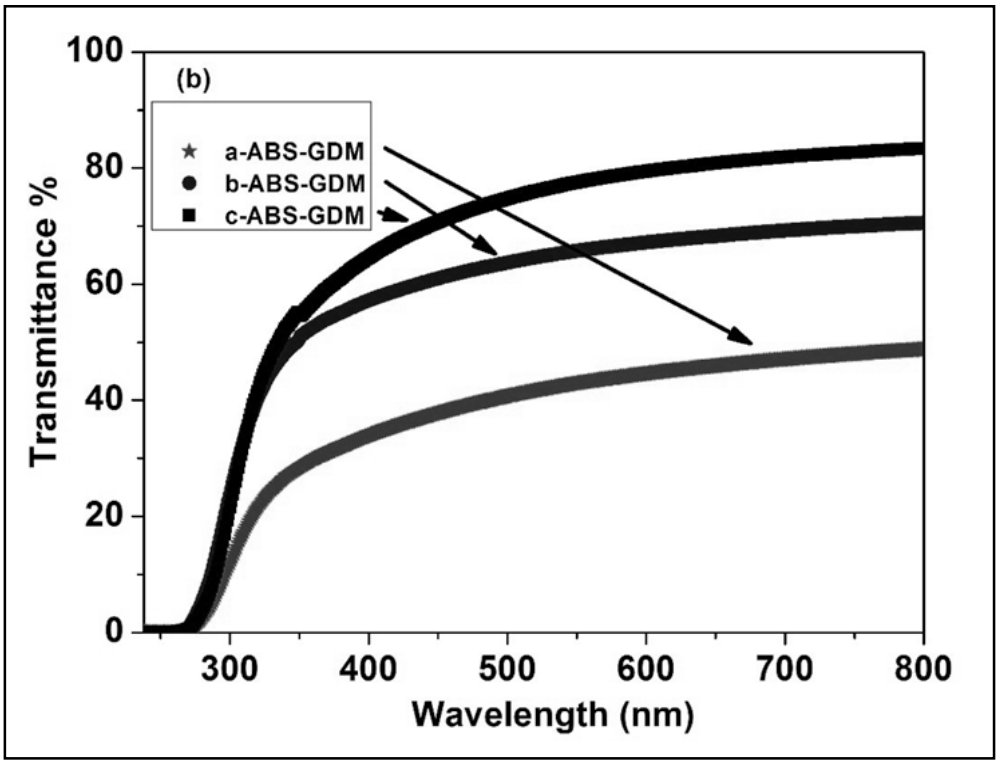

Fig. 7. (a) Absorption spectra of prepared ABS-GDM at different suspension concentrations. (b) Transmittance spectra of prepared ABS-GDM at different suspension concentrations (a-ABS-GDM (0.050 g/ml), b-ABS-GDM-25 (0.025 g/ml), and c-ABS-GDM (0.015 g/ml).

The transmittance spectra of the prepared ABS-GDM with different suspension concentrations are displayed in Fig. 7 (b). As seen in Fig. 7(b), the average transmittance values of the a-ABS-GDM, b-ABS-GDM, and c-ABS-GDM structures are 44%, 67%, and 80%, respectively, in the wavelength range of 400-800 nm. These results also show that transparency decreases with increasing additive material.

To determine the type of optical band gap from Fig. 4, we used the following relation [31-33]:

$$(\alpha h\nu) = A\,(h\nu - Eg)^{1/2} \qquad (1)$$

where ν h is the photon energy, and A is an energy-independent constant. Fig. 8 (a) shows the dependence of $(\alpha\nu h)^2$ versus photon energy ν (h) for the ABS-GDM structures. The predicted values of optical band gap were determined from Fig. 8 (a) and the optical band gap of the a-ABS-GDM, b-ABS-GDM and c-ABS-GDM structures were calculated to be 4.44 eV, 4.41 eV and 4.35 eV, respectively. The values of the optical energy gap (Eg) for the ABS-GDM structures are shown in Fig. 8(b). In this study, the ABS-GDM was successfully printed with the FDM device. Fig. 9 shows a 3D printed specimen from the ABS-GDM filaments.

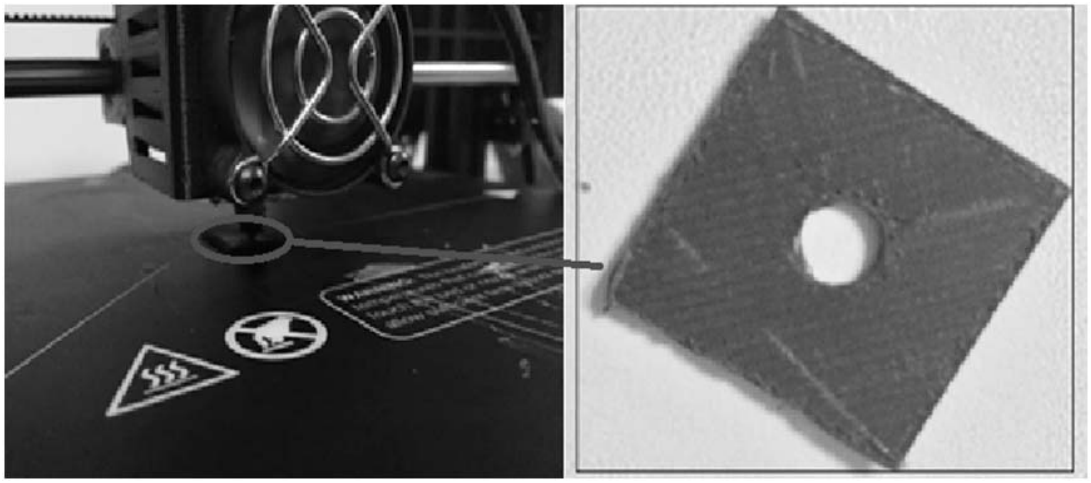

Fig. 9. Printed specimen from the ABS-GDM filaments.

4. CONCLUSIONS

In this study, ABS-GDM filaments with RGO and DBDPE were prepared by extrusion for FDM applications. The values of the optical band gap for the ABS-GDM structures ranged from 4.35 eV to 4.44 eV. It was also observed that the band gap energy decreases when optical average transmittance values increase. These results may be important for optoelectronic and photonic device applications. It was identified the functional groups of ABS-GDM using FTIR. As evident from the SEM images, RGO and DBDPE were homogeneously dispersed in the ABS polymer matrix. The flexural strength and the flexure modulus values of the ABS-GDM structures at room temperature were 53.74 MPa and 3051.41 MPa, respectively. The vertical combustion results show that ABS-GDM filaments can be a flame retardant with added RGO and DBDPE additives.T_g of the ABS-GDM filaments was found to be 104.256 °C. This is the first study where both RGO and DBDPE are used in pure ABS. The findings of our study suggest that this new generation of nanocomposite filaments with modified mechanical, thermal, and optical properties could be useful for FDM applications. The fabricated ABS-GDM filaments can be readily used in AM technology.

ACKNOWLEDGEMENTS

Part of this study was funded by Graf Nano Technological Materials Industry and Trade Ltd. Co. Also, we would like to thank Kahramanmaras Sütçü Imam University Scientific Research Projects Coordination Unit (Project No: 2018/3-6 YLS) for their financial supports.

References

1. L.J. Kumar, P.M. Pandey, D.I. Wimpenny (Eds.) 3D Printing and Additive Manufacturing Technologies" Springer Nat. Singapore Pte Ltd., 2019, XIV, 311 978-981-13-0304-3.
2. M. Jiménez, L. Romero, I.A. Domínguez, M. Del-M. Espinosa, M. and Domínguez, *Complex*ity, Article vol. 2019 (2019): 30.

3. B.E. Carroll, T.A. Palmer and A. M. Besse, *Acta Mater.* 87 (2015): 309.
4. E. Brandl, F.Palm, V. Michailov, B. Viehweger and C. Leyens, *Mater. Des.* 32 (2011): 4665.
5. P. Krawczak, *Exp Pol Lett* 9 (2015): 959.
6. D. Appleyard, *Met. Powder Rep.* 70 (2015): 285.
7. S. Hongyao, Y. Xiaoxiang and F. Jianzhong, *Int J Adv Manuf Technol* 97 (2018): 3205.
8. C.S. Lee, S.G. Kim, H.J. Kim and S. H. Ahn, *J Mater Process Technol* 187 (2007): 627.
9. M. Samykano, S.K. Selvamani, K. Kadirgama, W. K. Ngui, G. Kanagaraj and K. Sudhakar, *Int J Adv Manuf Technol* 102 (2019): 2779.
10. S. Stankovich, D.A. Dikin, G.H. B. Dommett, K.M. Kohlhaas, E.J. Zimney, E.A. Stach, R.D. Piner, S.T. Nguyen and R.S. Ruoff *Nature,* 442 (2006): 282.
11. T. Ramanathan, A. A. Abdala, S. Stankovich, D.A. Dikin, M. Herrera-Alonso, R.D. Piner, D.H. Adamson, H. C. Schniepp, X. Chen, R.S. Ruoff, S.T. Nguyen, I.A. Aksay, R.K. Prud'Homme and L.C. Brinson *Nat Nanotechnol,* 3 (2008): 327.
12. T. Kuilla, S. Bhadra, D.Yao, N.H. Kim, S. Bose and J.H. Lee, *Prog. Polym Sci,* 35 (2010): 1350.
13. N. Hill and M. Haghi, *Rapid Prototyp* J.20 (2014): 221
14. J.H. Shim, J.Y. Won, S.J. Sung, D.H. Lim, W.S. Yun, Y.C. Jeon and J. B. Huh, *Polymers.* 7 (2015): 2061.
15. S. Dul, L. Fambri and A. Pegoretti, *Compos: Part A* 85 (2016): 181.
16. M.A. Caminero, J.M.Chacón, E.García-Plaza, P.J. Núñez, J.M. Reverte and J.P. Becar, *Polym. J.* 11 (2019): 799.
17. M.A. Caminero, J.M. Chacón, I.Garcia-Moreno and J.M. Reverte, *Polym. Test.* 68 (2018): 415.

Received: 31-03-2021

Accepted: 16-09-2021

18. M.A. Caminero, J.M. Chacón, I. Garcia-Moreno and G.P. Rodriguez. *Compos. Part B* 148 (2018): 93.
19. C. Gonçalves, A. Pinto, A.V. Machado, J. Moreira, I.C. Gonçalves and F. Magalhães, *Polym. Compos.* 39 (2018): 308.
20. J. Bustillos, D. Montero, P. Nautiyal, A. Loganathan, B. Boesl and A. Agarwal, *Polym. Compos.* 39 (2018): 3877
21. C. Gonçalves, I. Gonçalves, F. Magalhães, A. Pinto, C. Gonçalves, I.C. Gonçalves, F.D. Magalhães and A.M. Pinto, *Polym. J. 9* (2017): 269.
22. I. Bayer and S.I. Bayer, *Materials* 10 (2017): 748.
23. J.M. Chacón, M.A. Caminero, P.J. Núñez, E. García-Plaza, I. García-Moreno and J.M. Reverte, *Compos Sci and Technol* 181 (2019): 107688.
24. J.M. Chacón, M.A. Caminero, P.J. Núñez and E. García-Plaza, *Mater. Des.* 124 (2017): 143.
25. İ. Karteri and M. Güneş, J Mater Sci: Mater Electron 27 (2016): 11502.
26. S.Urus, M. Caylar and I. Karteri, *Chem. Eng. J.* 306 (2016): 961.
27. J.G. Bokria and S. Schlick, *Polym.* 43 (2002): 3239.
28. C. Desrousseaux, R. Cueff, C. Aumeran, G. Garrait B. Mailhot-Jensen, O. Traoré and V. Sautou, *PLoS One.* 18 (2015): 0135632
29. K. Al-Ammar, A. Hashim and M. Husaien, *Chem. Mater. Eng.* 1 (2013): 85.
30. B. Neher, Md. M.R. Bhuiyan, H. Kabir, Md. A. Gafur and F. Ahmed, *Mater Sci Appl,* 9 (2018): 246.
31. K.R. Murali, A. Kalaivanan, S. Perumal and N. Neelakanda Pillai *J. Alloys Compd.,* 503 (2010): 350.
32. V. R. Shinde, T. P. Gujar, C. D. Lokhande, R. S. Mane and S. H. Han, *Mater. Chem. Phys.* 96 (2006): 326.
33. S. Urus, H. Adıguzel, M. Keles and I. Karteri, *Fuller Nanotub Car N* 25 (2017): 133.